Compact Wideband 5G SIW Bandpass Filter with Enhanced Selectivity Using Mixed-Coupling Butterfly CSRRs

Fatma Zohra HAMRIOUI [1], Rachida TOUHAMI [1, 2], Mohamad AL SABBAGH [3], Mustapha C. E. YAGOUB [3]

[1] Laboratoire des Dispositifs de Communication et de Conversion Photovoltaïque (LDCCP) Département d'Electronique, Ecole Nationale Polytechnique, Algiers, Algeria
[2] Instrumentation Laboratory, Faculty of Electronics and Informatics, USTHB University, Algiers, Algeria
[3] ELEMENT Laboratory, School of Electrical Engineering and Computer Science, University of Ottawa, Ottawa, Canada

fatma_zohra.hamrioui@g.enp.edu.dz

Submitted July 11, 2025 / Accepted December 10, 2025 / Online first January 26, 2026

Abstract. *In this work, a novel integrated waveguide bandpass filter for 5G applications is presented. The proposed compact filter is loaded by mixed coupling butterfly shaped complementary split ring resonators (B-CSRRs). Initially, the design exhibited only one transmission zero at higher stop-band. Thus, an asymmetric etched slot has been inserted between the split of each face-to-face B-CSRRs to produce an induced mixed coupling, thereby allowing the emergence of an additional transmission zero at lower stopband. To further improve the selectivity factor, a second-order SIW filter using two-mixed coupling face-to-face B-CSRRs, separated by a plus shaped ring slot resonator was designed. The measured results show good performance, including low insertion loss of 1.46 dB, high selectivity factor of 55.75%, compact size of 0.107λ_g^2 (with λ_g the guided wave at the center frequency f_c = 4.60 GHz), and high fractional bandwidth of 13.70% (i.e., 4.28–4.91 GHz). By covering the N79 5G band with a minimum attenuation of 40 dB from dc to 3.74 GHz and a minimum attenuation of 20 dB from 5.15 to 9.43 GHz, the proposed filter can be used for sub-6GHz 5G applications, as it prevents the interference between the N79 band and WiFi 5 GHz.*

Keywords

5G, complementary split ring resonators (CSRR), filter, selectivity factor, substrate integrated waveguide (SIW)

1. Introduction

Fifth generation (5G) mobile technology has recently been introduced for sub-6GHz radio systems [1] to meet the demand for higher data rates, higher capacity, and wider coverage. However, radio frequency (RF) interference and harmonic signals can provide significant challenges for current and upcoming wireless technology due to the proximity of 5G sub-6GHz band with 2.4- and 5-GHz Wi-Fi channels [2]. Thus, if an appropriate filtering process is not performed, data rates may be significantly impacted, and hardware damage may result [2]. Therefore, 5G filters are gaining an even-increasing interest from researchers. In designing planar bandpass filters, several key parameters have to be considered such as the number of poles and zeros, the fractional bandwidth, the factor of selectivity, the attenuation rate at the rejection band, as well as the filter shape.

Substrate Integrated Waveguide (SIW) technology, which combines the features of planar circuits and waveguides, such as low loss, high performance, and good planar integration [3], has been offered as a suitable technique to design filters in order to compromise between low cost and high performance. Therefore, a single-band SIW bandpass filter (BPF) was synthesized on a planar substrate with periodic linear arrays of metalized vias, making it compatible for integration with printed circuit boards [3]. Then, in [4], a dual-mode SIW filter was designed using a square cavity. Based on via perturbation the proposed approach offers adjustable Transmission Zeros (TZs) while maintaining SIW integrity and shielding without increasing design complexity. In [5], quarter-mode (QM) and eighth-mode substrate integrated waveguide cavities were analyzed and applied to design filters in order to further minimize the size of the cavity as well as enhance the performance of SIW filters in terms of selectivity and creating extra transmission zeros. In [6], a different approach of designing bandpass filter using an isosceles right-triangle SIW cavity has been discussed. This cavity is supported by two T-shape stub-loaded resonators to generate a transmission zero at the lower stopband, as well as a Complementary Split Ring Resonator (CSRR) etched on the SIW's ground plane, which produces two controllable transmission zeros at the upper stopband. In [7], a high-selective double-mode SIW bandpass filter utilizes Modified Parallel Coupled Microstrip Lines (MPCML) between source and load to form TZs, as well as improving out-of-band performance. The passband of this filter has

DOI: 10.13164/re.2026.0095

been generated by perturbing the TE_{101}- and TE_{102}- modes with metallic vias. A size reduction can be achieved as well for a SIW filter based on D-shaped CSRRs, as described in [8]. This filter exhibits a compact size and a good wide-out-of-band rejection up to 20 GHz.

Nevertheless, the above works have some limitations, such as large size [4, 6, 7], design complexity [5], or exhibiting only one transmission zero at the higher stop band [8].

In this paper, a novel, selective, and compact SIW bandpass filter based on loaded mixed coupling Butterfly shaped Complementary Split Ring Resonators (B-CSRRs) is proposed. The second-order response of the proposed filter is generated by merging two stages of face-to-face mixed coupling B-CSRRs separated by a Plus shaped Ring Resonator (PRR). PRR is novel approach proposed in this paper to enhance the in-band flatness by combining the dominant mode generated by the joined face-to-face B-CSRRs, referred to as the asymmetric continuous-coupled dual B-CSRR, and the conventional CSRR mode under one desirable pass-band while maintaining compact size, high selectivity response, and wide bandwidth.

Unlike the conventional CSRRs, SIW bandpass filters have only TZs on the upper stop-band, so the asymmetric continuous-coupled dual B-CSRR generates a mixed coupling, which subsequently introduces a transmission zero at lower stop-band. In the other hand, the etching PRR in the middle of the SIW cavity controls the position of the conventional CSRR mode, providing a flat pass-band with high selectivity and simultaneously reducing the filter size. The proposed filter demonstrates excellent performance including compact size of 0.107 λ_g^2 (where λ_g represents the guided wavelength at the center frequency f_c = 4.60 GHz), high selectivity factor of 55.75%, and low insertion loss of 1.46 dB while covering the entire N79 band (4.4–5.0 GHz) with 20 dB rejection in the range of 5.15–9.43 GHz, thus preventing possible interference with the 5 GHz WiFi band.

2. Design Methodology

Based on printed circuit board (PCB) technology, a substrate-integrated waveguide was synthesized on a planar substrate using linear periodic arrays of metallized vias. It uses 0.79 mm thick Rogers RT/Duroid 5880 substrate with permittivity of 2.2 and dielectric loss tangent of 0.0009. Incorporating CSRRs in a SIW cavity allows creating an additional pass-band below the waveguide cutoff in accordance with the theory of evanescent-mode propagation [9]. The methodology approach was to enhance selectivity through a series of design strategies, starting from a single-stage filter to a mixed coupling to a two-stage design to, ultimately, a plus shaped slot-based merging modes technique is introduced to reach a uniform pass-band (i.e., optimized flatness and reduced insertion loss over broadened bandwidth) while maintaining the overall dimensions. All these techniques are well detailed in the following sections. Note that all aspects of the structure's design and electromagnetic simulations were conducted using CST Studio Suite.

2.1 Characteristics of Butterfly B-CSRR Resonators in SIW Technology

As a brief reminder, an SIW is a planar implementation of a rectangular waveguide, achieved by embedding metallic vias in a dielectric substrate. The substrate's top and bottom surfaces form the waveguide walls, while the via arrays define the sidewalls. The effective dimensions of the SIW, considering the via diameter (d) and spacing (s) [10], are:

$$W_{\text{eff}} = W - \frac{d^2}{0.95s}. \tag{1}$$

The operating frequency range is primarily defined by the cutoff frequency of the quasi-TE_{10} mode, which depends on the effective width W_{eff}. Due to the via discontinuities, only the TE mode can propagate in the SIW, as the TM mode cannot establish a stable current along the metalized via sidewalls. The SIW cutoff frequency f_c of the first mode can be calculated by [10]:

$$f_{c(\text{TE}_{10})} = \frac{c}{2 \times W_{\text{eff}} \sqrt{\varepsilon_r}} \tag{2}$$

where c is the velocity of light and ε_r the substrate relative permittivity.

The design procedure for the suggested filter is summarized below:

- Initially, a SIW rectangular cavity with a width of 13.30 mm is chosen to operate at the fundamental mode, having a cutoff frequency of 7.84 GHz as defined by (2). To minimize leakage loss, the diameter d and pitch s of the via holes are selected appropriately such as

$$\frac{d}{\lambda_g} \le 0.1 \text{ and } \frac{d}{s} \ge 0.5. \tag{3}$$

  Note that a 50 Ω microstrip line is used to feed the input and output ports.

- To achieve a pass-band filtering response, face-to-face butterfly-shaped CSRRs are introduced on the top layer of the SIW cavity. This configuration produces a pass-band around 5.12 GHz below the cutoff frequency, in accordance with the theory of evanescent-mode propagation, and includes a transmission zero in the upper stop-band.

- To improve the selectivity of the filter, an asymmetric continuous-coupled dual butterfly-CSRR is developed, where the two previous face-to-face butterfly-CSRRs are linked by an asymmetrically placed slot. The goal of this configuration is to enhance the filter's steepness by producing a transmission zero at the lower stop-band through mixed coupling between the face-to-face butterfly-CSRRs. Moreover, it improves the compactness by shifting the pass-band to a lower frequency of 4.64 GHz without changing the overall dimensions.

- To further enhance the selectivity, the number of stages can be increased; however, it results in a non-flat pass-band and high insertion loss. Therefore, to achieve a uniform pass-band with optimized flatness and reduced insertion loss over a broadened bandwidth, a Plus shaped Ring Resonator (PRR) is introduced between the stages, where the goal of a uniform broadband pass-band filter with high selectivity is achieved to full-fill the 5G requirements.

Figure 1 illustrates the design evolution of the designed butterfly CSRR SIW topology. As demonstrated in Fig. 1(b), the first topology (Prototype 1) allowed the cavity SIW filter to exhibit high-pass filter characteristics, with a cutoff frequency inversely proportional to the width (W_s). By introducing the conventional rectangular complementary split-ring resonators (CSRRs) into the SIW structure, a pass-band was generated below the cutoff frequency (Prototype 2). Further tuning the filter's response can be achieved by transforming the rectangular CSRRs into butterfly CSRRs (Prototype 3). This modification shifts the first transmission zero from 8.5 GHz to 7 GHz while slightly shifting the passband to a higher frequency. In other words, the butterfly B-CSRRs exhibit a steeper roll-off at the upper stop-band compared to the conventional CSRRs, indicating a more selective response.

A parametric study on the final prototype, depicted in Fig. 2, reveals that parameters l_3 and n_1 have a substantial impact on the filter's frequency response, particularly the passband and transmission zero locations, demonstrating the tunability of the filter. Therefore, while the adopted shape could be seen as 'unusual' and regular shapes could be preferred, the novel butterfly-shaped configuration offers enhanced control over the first transmission zero, enabling improved selectivity in the desired frequency range. Additionally, the butterfly shape effectively manages the coupling between stages, ensuring optimal performance even when increasing the filter order.

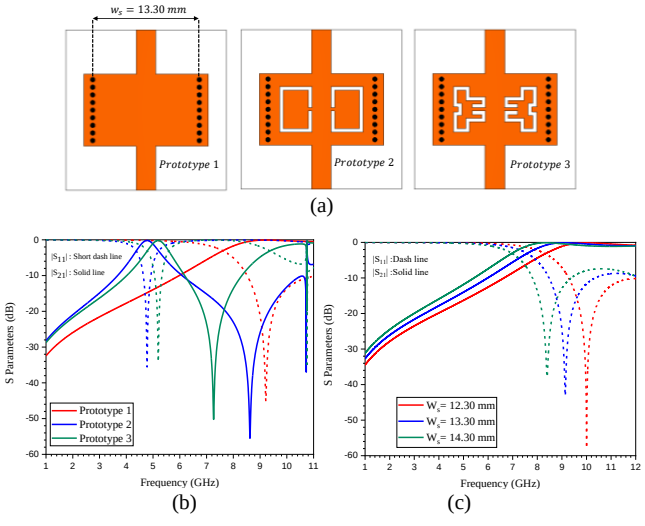

Fig. 1. Design evolution towards butterfly CSRRs topology: (a) Prototypes; (b) Comparison of simulated S-parameters among different prototypes; (c) Variation of S-parameters with respect to W_s (prototype 1).

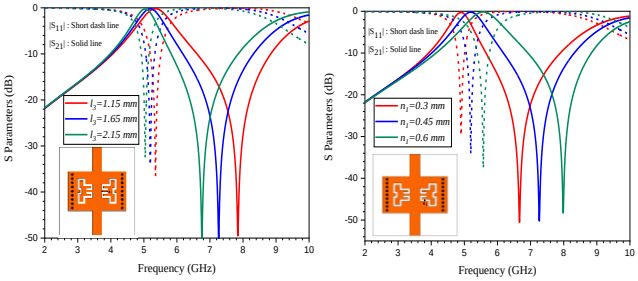

Fig. 2. Variation of S-parameters with respect to (a) l_3, (b) n_1.

2.2 First Order SIW Bandpass Filter Based on Asymmetric Continuous-Coupled Dual B-CSRRs

The design of the filter starts with a first order SIW device based on loaded B-CSRRs (Prototype 3, Fig. 3a). Involving two face-to-face butterfly-shaped CSRRs with no link slot between them, it operates at 5.19 GHz with a selective factor of 17.13 % and only one transmission zero at 7.26 GHz (Fig. 3b).

Whereas as the splits of the two face-to-face B-CSRRs are continuously joined by an asymmetrically placed slot (Prototype 4, Fig. 3a) a mixed coupling is induced. Thus, a new transmission zero is generated at 2.28 GHz in the lower stop-band (Fig. 3b). Consequently, the selective factor and the FBW are both enhanced to 37.13% and 17.65%, respectively, achieving a wide rejection band with a minimum attenuation of 49 dB from dc to 2.52 GHz in the lower stop-band and 20 dB attenuation at higher stop-band up to 7.27 GHz.

Note that the splits of both face-to-face B-CSRRs should be continuously joined by an asymmetric slot not just to create a transmission zero at lower stop-band but also to preserve the operating pass-band. If a symmetric slot is created between the CSRRs, in addition to the transmission zero generated at lower stop-band, the operating pass-band will be attenuated. In fact, the symmetric slot prevents the electric field from flowing from one port to another whereas is not the case in asymmetric slot.

The equivalent circuit models for the single stage SIW filter loaded by B-CSRRs (with and without asymmetric etched slot) are shown in Fig. 3(b). In both models, a parallel inductor L_{vias} models the row metallic via in SIW. A series shunt resonator, formed by an inductor L_c and a capacitor C_c, represents the external coupling between the SIW and the resonators. The face-to-face CSRRs are modeled by two parallel shunt resonant tanks formed by a capacitor C_r and an inductor L_r. However, in the fourth prototype, another series shunt resonator formed by L_s and C_s has been introduced between the two B-CSRRs to represent the mixed coupling induced by the asymmetric continuous dual B-CSRRs. Electrical parameters of prototype 3 equivalent circuit are: L_{via} = 3.08 nH, L_c = 0.6 nH, C_c = 0.81 pF and C_r = 1.54 pF. These values are also the same for prototype 4, except that C_r = 1.67 nH and with L_s = 10.9 nH and C_c = 0.44 pF.

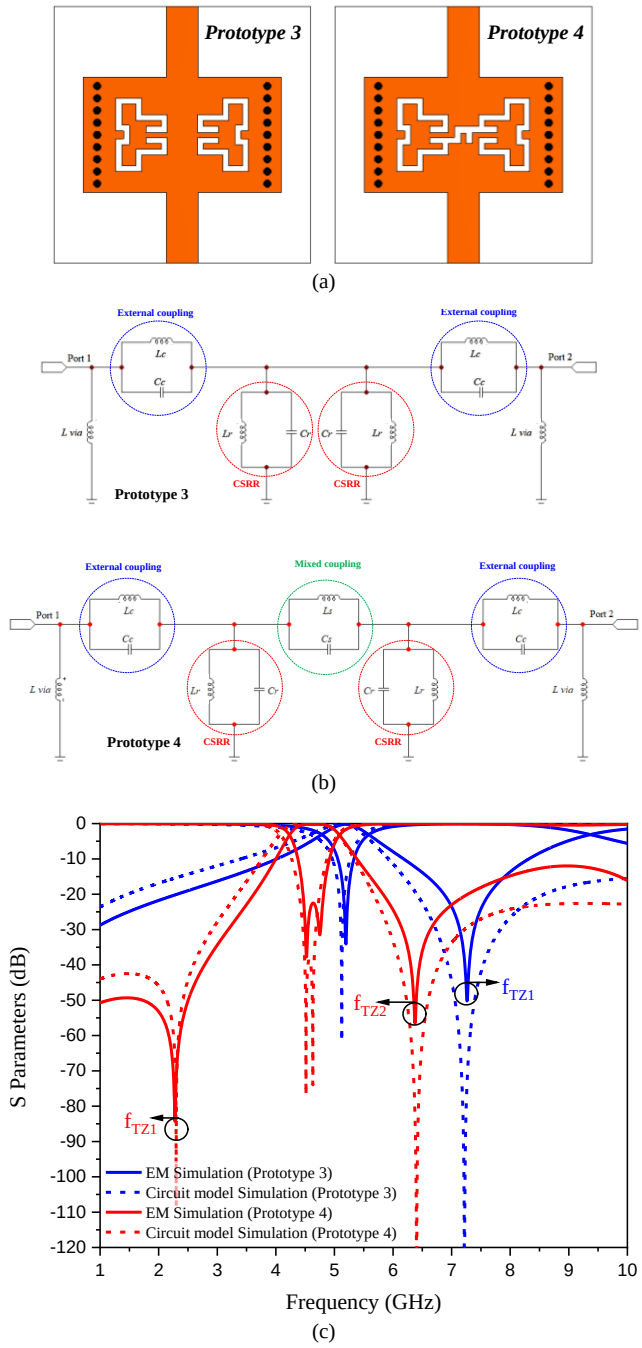

Fig. 3. First order SIW bandpass filter based on B-CSRRs: (a) Prototypes; (b) Equivalent circuits; (c) Simulated S-parameters.

It is worth mentioning that the loaded CSRRs act as electric dipoles [9] whose resonance frequency is related to size. Therefore, changing the CSRR dimensions will influence the operating band as [11], [12]:

$$f_r = \frac{1}{2\pi\sqrt{L_r C_r}}. \tag{4}$$

It is found that the external coupling between the SIW and resonators can produce a transmission zero at the upper stop band of the proposed filter, at frequency f_{z1} given by [12]:

$$f_{z1} = \frac{1}{2\pi\sqrt{L_c C_c}}. \tag{5}$$

Whereas the mixed coupling between the two connected B-CSRRs (i.e., Prototype 4) can produce a transmission zero at the lower stop band [12] as:

$$f_{z2} = \frac{1}{2\pi\sqrt{L_s C_s}}. \tag{6}$$

The design structure of the proposed single stage SIW bandpass filter based on asymmetric continuous-coupled dual B-CSRRs, along with its dimensions, is illustrated in Fig. 4. This proposed filter has been designed using 0.79 mm thick Rogers RT/Duroid 5880 substrate, which exhibits a relative permittivity ε_r of 2.2 and a dielectric loss tangent (tanδ) of 0.0009. The physical dimensions are given in Tab. 1.

The impact of increasing parameter l_3 is shown in Fig. 5(a). It can be seen that as l_3 is increased, the transmission zero at the lower pass-band remains fixed, while the

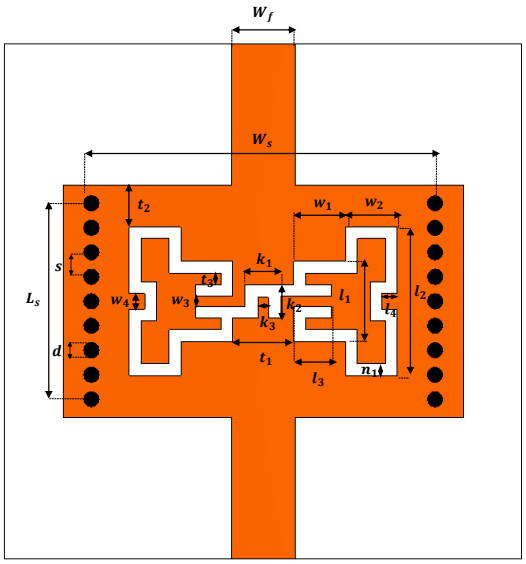

Fig. 4. Geometric structure of the proposed single-stage SIW bandpass filter based on asymmetric continuous-coupled dual B-CSRRs.

Parameter	Values (mm)	Parameter	Values (mm)
W_s	13.30	n_1	0.45
L_s	8.00	t_1	2.37
w_1	2.00	t_2	2.88
w_2	2.00	t_3	0.45
w_3	0.40	s	0.95
w_4	0.60	d	0.60
l_1	3.10	k_1	1.40
l_2	5.75	k_2	1.30
l_3	1.45	k_3	0.40
l_4	0.60		

Tab. 1. Physical dimensions of the proposed single stage band pass SIW filter based on asymmetric continuous-coupled dual B-CSRRs in (mm).

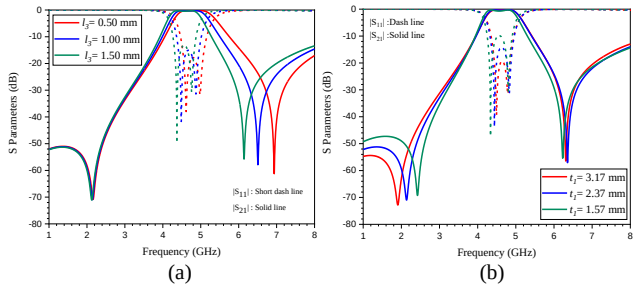

Fig. 5. Simulated S parameters of the suggested single stage SIW bandpass filter and its parametric results by varying (a) l_3, (b) t_1.

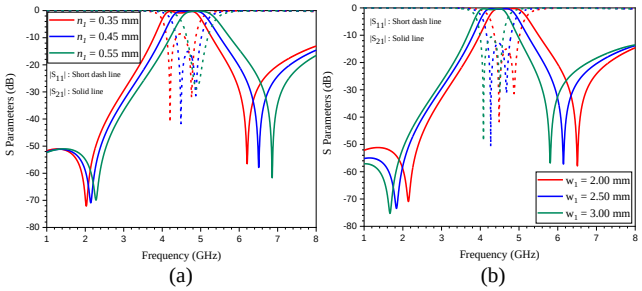

Fig. 6. Simulated S parameters of the suggested single stage SIW bandpass filter and its parametric results by varying (a) n_1, (b) w_1.

transmission zero at the upper pass-band moves toward a lower frequency, increasing the steepness of the upper stop-band. The effect of increasing parameter t_1 is shown in Fig. 5(b). As t_1 is increased, the transmission zero at lower pass-band is moved toward a higher frequency, while the transmission zero at the upper pass-band remains almost fixed. Note that the return loss within the center of the pass-band is reduced with an increase in t_1.

The impact of increasing parameter n_1 is shown in Fig. 6(a). It can be seen that as n_1 is increased, both transmission zeros move toward a higher frequency, with more significant variation for the transmission zero at the upper pass-band compared to the lower pass-band. The pass-band is also shifted to a higher frequency, and the two modes within the pass-band approach each other. As w_1 is increased, as illustrated in Fig. 6(b), both the transmission zeros and the pass-band shift toward lower frequencies. This is due to the increase in the electrical length of the CSRRs as w_1 is increased.

2.3 Second Order SIW Bandpass Filter Based on Asymmetric Continuous-Coupled Dual B-CSRRs Separated by PRR

In order to further improve the selectivity factor of the proposed filter, a double stage of mixed coupling B-CSRRs was then proposed, as shown in Fig. 7(a), with W_s = 14.16 mm, L_s = 17.10 mm, and q = 9.80 mm. From Fig. 7(b), we can see that the filter response becomes more selective after increasing the number of stages with selectivity factor of 71%. Both lower and higher stop-band rejections are now improved where an attenuation of 74 dB is observed in the lower stop band and an attenuation of 20 dB is observed at higher stop-band up to 8.35 GHz. Also, a significant distortion in the in-band is observed due to the coupling between the two stages. In fact, two modes are detected: one at 4.40 GHz and the second one at 5.35 GHz, creating high insertion and low return loss at frequency of 5.13 GHz within the pass-band.

To highlight that phenomenon, the electric field distribution at the first mode (i.e. 4.40 GHz) and the second mode (i.e. 5.35 GHz) are depicted in Fig. 8. At mode 1, the electric field distribution is mainly centered at the joined face-to-face B-CSRRs, whereas, at mode 2, the electric field is distributed on the edges of the B-CSRRs and almost zero around the etched slots between each face-to-face B-CSRRs. Thus, the first mode is generated by asymmetric continuous-coupled dual B-CSRRs, whereas the second mode is the dominant mode of the conventional B-CSRRs (i.e., without any joined slot). Note that the electric field distribution revealed a notably weaker interaction in the region between the stages at both modes. This weakness likely contributed to the inadequate filter response, characterized by a non-flat pass-band and poor return loss and insertion loss at the center frequency.

Since the proposed structure is a symmetric double stage SIW filter, the external quality factor Q_e can be de-

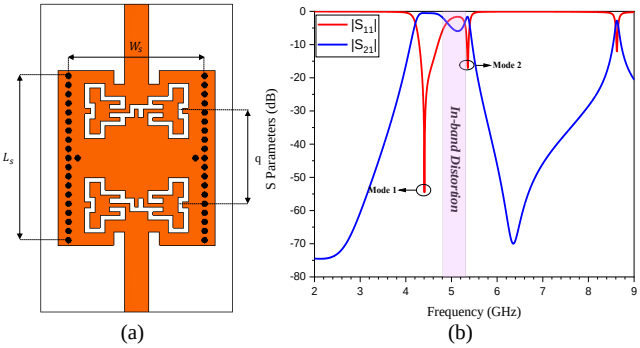

Fig. 7. Double stage SIW filter using mixed-coupling B-CSRRs: (a) Prototype; (b) Simulated S-parameters.

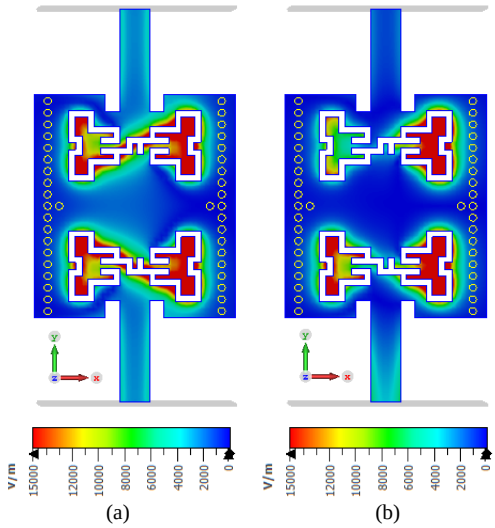

Fig. 8. Electric field distribution at: (a) Mode 1: 4.40 GHz; (b) Mode 2: 5.35 GHz.

rived by simulating the double loaded resonator and is then calculated as follows [8], [9]:

$$Q_e = \frac{2 f_0}{\Delta f_{3dB}} \tag{7}$$

where f_0 is the frequency at which the parameter S_{21} reaches its maximum value and $\Delta f_{3\,dB}$ is the bandwidth for which the attenuation of S_{21} is 3 dB from its maximum value. The unloaded quality factor is then calculated as follows [13]:

$$Q_u = \frac{10^{\frac{|S_{21}|}{-20}} Q_e}{1 - 10^{\frac{|S_{21}|}{-20}}}. \tag{8}$$

As for the selectivity factor (SF) of the proposed filter, it can be computed as [8]:

$$SF(\%) = \frac{\Delta f_{3dB}}{\Delta f_{20dB}} \times 100. \tag{9}$$

Figure 9 displays the effect of increasing the distance q between the stages on the S-parameters, insertion loss and return loss at the center frequency, the lower and higher modes, the unloaded quality factor, the selectivity factor, and the size of the filter. Note that increasing q implies increasing the length of the SIW cavity; thus, the study is based on the factor L_s/λ_g. It can be seen from that figure that as q is increased, the unloaded quality factor is increased whereas the selectivity factor is reduced. The lower mode is moved toward higher frequency and higher mode is moved toward lower frequency while the size of the filter is increased. Note that in order to get a nearly flat in-band performance, i.e., an insertion loss less than 3 dB and a return loss higher than 10 dB, q should exceed 15.80 mm. However, it will be at the expense of a larger L_s (larger than 0.52 λ_g) while the selectivity factor and the FBW should not exceed 35% and 8.9%, respectively.

Therefore, in order to achieve an almost flat pass-band with low insertion loss while keeping the filter size as compact as possible and the selectivity factor as high as feasible, a Plus shaped Ring Resonator (PRR) is introduced between

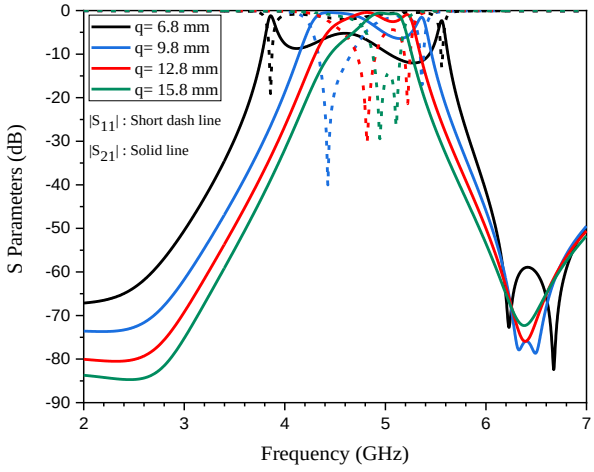

(a)

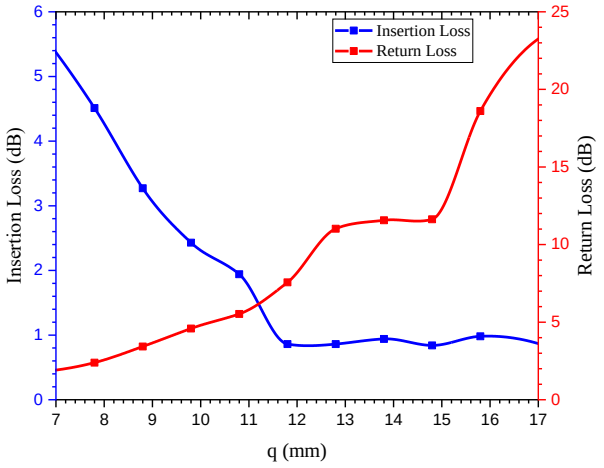

(b)

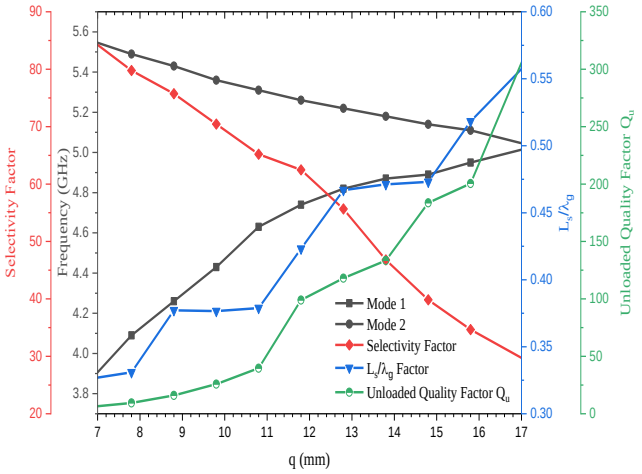

(c)

Fig. 9. Effect of the parameter q on (a) S-parameters, insertion loss and return loss at the center frequency; (b) modes, unloaded quality factor, selectivity factor and size.

Parameter	**Values** (mm)	**Parameter**	**Values** (mm)
W_s	14.16	n_1	0.50
L_s	17.10	n_2	0.40
w_1	2.10	t_1	2.37
w_2	2.10	t_2	1.32
w_3	0.40	t_3	0.35
w_4	0.60	s	0.95
l_1	3.10	d	0.60
l_2	5.75	x_1	1.16
l_3	1.60	y_1	1.40
l_4	0.60	m_1	1.60
k_1	1.40	m_2	3.75
k_2	1.40	m_3	1.60
k_3	0.40	m_4	2.40
q	9.80		

Tab. 2. Geometric dimensions of the proposed double stage SIW bandpass filter based on asymmetric continuous-coupled dual B-CSRRs separated by PRR (in mm).

the two stages, with q = 9.80 mm. Figure 10(a) shows the final structure of selective double stage SIW bandpass filter based on loaded asymmetric continuous-coupled dual B-CSRRs separated by PRR, the geometric dimensions are given in Tab. 2 and the equivalent circuit model is given in Fig. 10(c).

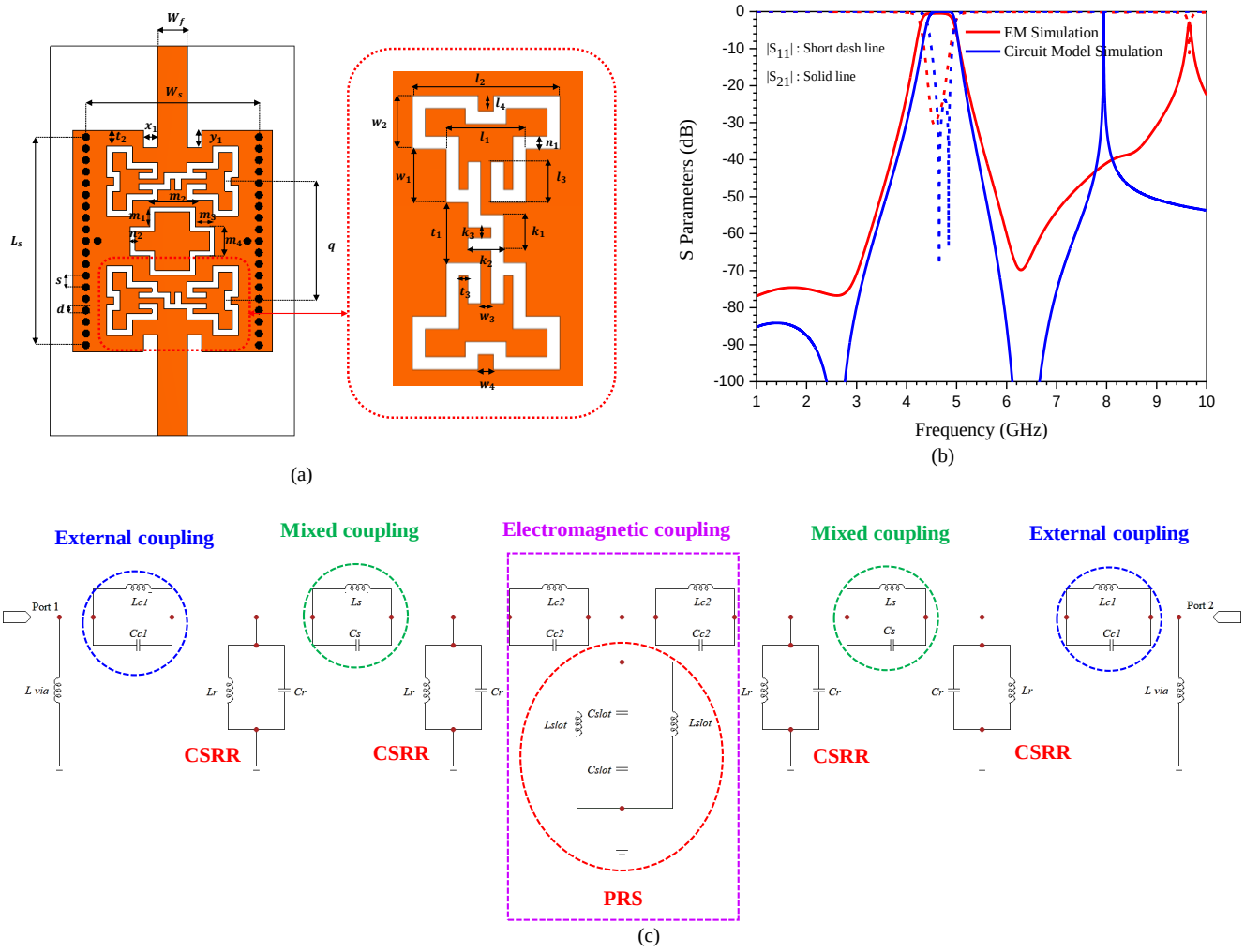

Fig. 10. The final structure of the proposed SIW bandpass filter: (a) Layout; (b) S-parameters from both EM simulation and circuit model; (c) The equivalent circuit.

Asymmetric continuous-coupled dual CSRRs are modeled by two parallel shunt resonant tanks (C_r and L_r). Their primary resonant frequency f_r is given by (4).The mixed coupling between the two joined CSRRs is represented by a series shunt resonator (L_s, C_s). The transmission zero generated by this mixed coupling is determined by (6) and is responsible for shaping the filter's lower stop-band edge. The external coupling between the Substrate Integrated Waveguide (SIW) and the CSRRs is modeled by a series shunt resonator (L_{c1}, C_{c1}). This element is responsible for generating the transmission zero in the upper stop-band, as defined by (5).The coupling between the two stages is additionally represented by two series shunt resonators (L_{c2}, C_{c2}). The transmission zero associated with these elements is also governed by (5). These two elements are specifically used to improve the selectivity at upper stop-band. These two shunt resonators are separated by the equivalent circuit modeling of PRR (i.e., L_{slot} and C_{slot}) [14]. The numerical values for all components were optimized in the Advanced Design System (ADS) software. This optimization procedure ensured that the S-parameters of the equivalent circuit model precisely matched the S-parameters obtained from the full-wave electromagnetic simulation of the physical structure. Following this, the Plus shaped Ring Resonator (PRR) parameters, L_{slot} and C_{slot}, were further optimized to achieve the target uniform pass-band response (improved flatness, reduced insertion loss, and a broadened bandwidth) by controlling the modes variation within the pass-band without significantly affecting the filter's performance outside the pass-band. The electrical parameters of the suggested double stage SIW bandpass filter based on mixed coupling B-CSRRs separated by PRR are: $L_{via} = 4$ nH, $L_{c1} = 0.5$ nH, $C_{c1} = 1.27$ pF, $L_r = 0.81$ nH, $C_r = 1.69$ pF, $L_s = 10.9$ nH, $C_s = 0.34$ pF, $L_{c2} = 0.8$ nH, $C_{c2} = 0.77$ pF, $L_{slot} = 1.6$ nH and $C_{slot} = 0.1$ pF.

Figure 10(b) shows the S-parameters obtained by electromagnetic (EM) simulation and equivalent-circuit model simulation.

The EM simulation and the circuit model show strong agreement. They share several essential frequency points, such as the resonant frequency, the transmission zeros, and the pass-band response, except for the location of the first harmonic that appears at 8 GHz instead of 9.80 GHz. EM simulation shows that the filter exhibits almost flat pass-band with selectivity factor of 56% after inserting the PRR between the two stages with two transmission zeros at 2.60 GHz and 6.29 GHz, respectively.

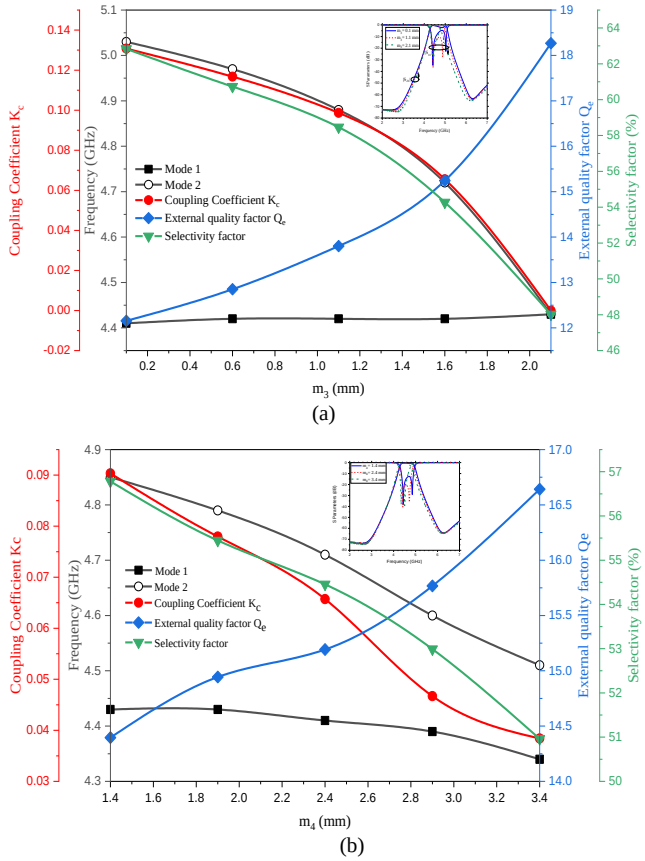

Fig. 11. Variation of mode 1 and mode 2, coupling coefficients, external quality factor and selectivity factor with respect to (a) m_3; (b) m_4.

To better highlight the relationship between the PRR physical dimensions and the filter performance, the impact of the dimensions m_3 and m_4 on the coupling coefficient, external quality factor, and selectivity factor are shown in Figs. 11(a) and (b), respectively. As m_3 increased, the higher mode is moved toward lower frequencies, whereas the lower mode is almost unchanged, resulting in an improvement in the external coupling coefficient and a significant reduction in the selectivity factor. The same behavior is observed when m_4 is increased, except that the higher mode is slightly moved toward a lower frequency and the selectivity factor is slightly reduced. Thus, what can be deduced is that the PRR has a main control over the conventional B-CSRR mode without affecting the mode of the mixed coupling B-CSRRs.

Note that the coupling coefficient K_c of the proposed filter can be extracted using the following relation [8], [9]:

$$K_c = \frac{f_2^2 - f_1^2}{f_2^2 + f_1^2}. \tag{10}$$

3. Fabrication and Measurements

The double stage SIW filter based on loaded mixed coupling B-CSRRs and separated by PRR was constructed using a 0.79 mm thick Rogers RT/Duroid 5880 substrate, which exhibits a relative permittivity ε_r of 2.2 and a dielectric loss tangent (tanδ) of 0.0009. The suggested filter has a footprint of 14.16 mm × 17.10 mm ($0.298\,\lambda_g \times 0.360\,\lambda_g$, where λ_g represents the guided wavelength at the center frequency of 4.60 GHz). The fabricated filter and its measurement bench are displayed in Figs. 12 and 13, respectively. The comparison between the simulated and measured S-parameters for the fabricated filter is presented in Fig. 14.

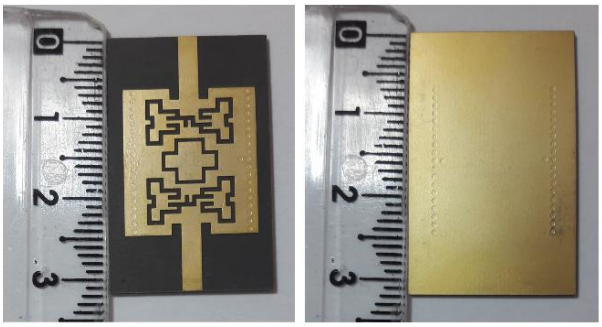

Fig. 12. Photograph of the fabricated SIW bandpass filter based on asymmetric continuous-coupled dual B-CSRRs separated by PRR: (a) Top view; (b) Back view.

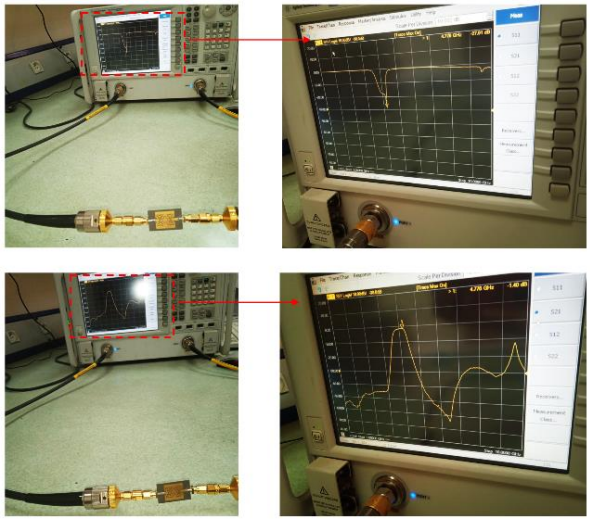

Fig. 13. Vector Network Analyzer testing of the fabricated filter's S-parameters.

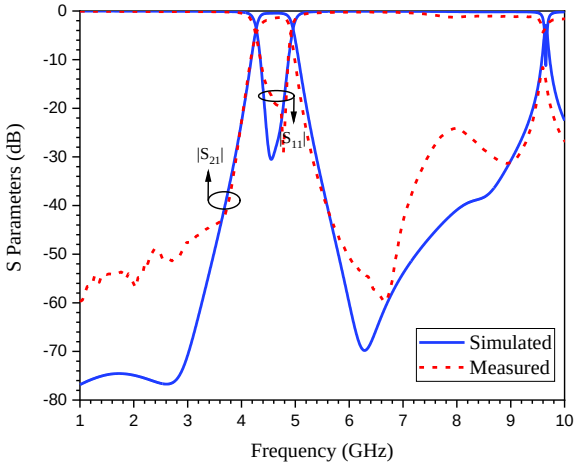

Fig. 14. Comparison of simulated and measured S-parameters of the fabricated filter.

Ref.	f_c (GHz)	–3 dB FBW (%)	IL (dB)	RL (dB)	Upper stop-band $\|S_{21}\| \le -20$ dB	SF (%)	Size (λ_g^2)
[4]	15.00	4.30	1.70	-	$1.29f_c$	54.80	2.761
[5]	3.09	15.20	1.34	15.00	$2.56f_c$	49.75*	0.292
[6]	8.98	15.90	0.90	20.00	$1.28f_c$	53.71	1.513
[7]	14.39	5.56	1.60	15.00	-	53.33*	0.427
[8]	6.11	8.96	1.07	20.00	$3.27f_c$	32.22	0.116
[15]	8.00	5.00	1.70	11.00	$1.60f_c$	17.50	0.09
[16]	8.00	3.51	2.15	-	-	47.17	0.798
[17]	11.51	6.78	1.42	13.00	$1.28f_c$	74.00*	0.504
[18]	8.50	6.11	1.70	-	$2.04f_c$	65.00*	1.155
[19]	6.97	1.98	2.28	12.10	$1.08f_c$	39.50*	0.122
[20]	10.00	11.30	0.90	-	$2.23f_c$	48.10*	0.282
This work	**4.60**	**13.70**	**1.46**	**19.00**	$\mathbf{2.05}f_c$	**55.75**	**0.107**

Tab. 3. Performance comparison of the proposed filter with existing works. (*: Estimated).

The simulated and measured results show strong agreement, with only a minor deviation due to SMA connector loss (probably due to some radiation or surface mode effects because of their grounding pins) as well as manufacturing tolerances.

The measured Insertion Loss (IL) within the passband is about 1.46 dB, while the Return Loss (RL) is greater than 19 dB. The measured fractional bandwidth (FBW) of bandpass filter is around 13.70% (i.e., 4.28–4.91 GHz), covering the entire N79 5G band. The measured stopband rejection level at the lower side of passband is greater than 40 dB from dc to 3.74 GHz, with one transmission zero generated at 2.70 GHz with an attenuation of 51.50 dB, while the stopband rejection at the higher stop band is better than 20 dB from 5.15 to 9.43 GHz (2.05 f_c), with two transmission zeros at 6.67 GHz and 8.95 GHz (with respective attenuations of 59.9 dB and 21.20 dB), giving good suppression for WIFI 5 GHz, with a selectivity factor (SF) of 55.75% and unloaded quality factor of $Q_u = 79.77$.

The performance comparison between the fabricated filter and existing works is summarized in Tab. 3. With a low complexity design, the proposed work has the highest FBW, high selectivity factor, and compact size compared to most reported works.

4. Conclusion

This paper proposed a novel compact selective SIW bandpass filter loaded by a pair of mixed coupling face-to-face butterfly shaped B-CSRRs separated by PRR. With asymmetric continuous-coupled dual B-CSRRs, a mixed coupling has been induced thus, generating a transmission zero at the lower stop band. By etching PRR between the merging stages of face-to-face mixed coupling B-CSRRs, an almost flat pass-band response is achieved. PRR can control the conventional CSRRs mode without significantly impacting the joined B-CSRRs mode. Furthermore, it ensures a high selectivity factor of 55.75% with reduced size. The measured results are in good agreement with the simulations, The fabricated filter demonstrated excellent performance in terms of out-band rejection up to 2.05 f_c, compact size of 0.107 λ_g^2, low insertion loss of 1.46 dB, high selectivity factor of 55.75%, and wide bandwidth (from 4.28 to 4.91 GHz), making it suitable for 5G applications.

References

[1] MONTAZEROLGHAEM, M. A., DE VREEDE, L. C. N., BABAEIE, M. A highly linear receiver using parallel preselect filter for 5G microcell base station applications. *IEEE Journal of Solid-state Circuits*, 2023, vol. 58, no. 8, p. 2157–2172. DOI: 10.1109/JSSC.2023.3267723

[2] ELECTRONIC DESIGN. *5-GHz Wi-Fi Coexistence with 5G Cellular Improves the User Experience.* [Online] Cited 2025-03-12. Available:https://www.electronicdesign.com/technologies/analog/article/21125072/5-ghz-wi-fi%20coexistence-with-5g-cellular-improves-the-user-experience

[3] LIU, J., JACKSON, D. R., LONG, Y. Substrate integrated waveguide (SIW) leaky-wave antenna with transverse slots. *IEEE Transactions on Antennas and Propagation*, 2012, vol. 60, no. 1, p. 20–29. DOI: 10.1109/TAP.2011.2167910

[4] CHU, P., HONG, W., TUO, M., et al. Dual-mode substrate integrated waveguide filter with flexible response. *IEEE Transactions on Microwave Theory and Techniques*, 2017, vol. 65, no. 3, p. 824–830. DOI: 10.1109/TMTT.2016.2633346

[5] LI, P., CHU, H., CHEN, R. Design of compact bandpass filters using quarter-mode and eighth-mode SIW cavities. *IEEE Transactions on Components, Packaging and Manufacturing Technology*, 2017, vol. 7, no. 6, p. 956–963. DOI: 10.1109/TCPMT.2017.2677958

[6] GUO, H., AN, X., LV, Z. Dual-mode bandpass substrate integrated waveguide filter with a complementary split ring resonator. *Microwave and Optical Technology Letters*, 2018, vol. 60, no. 3, p. 735–741. DOI: 10.1002/mop.31039

[7] YIN, B., HUANG, Q., HAO, H., et al. A high-selectivity double-mode SIW bandpass filter utilizing the modified parallel coupled microstrip lines. *Electromagnetics*, 2021, vol. 41, no. 4, p. 263–274. DOI: 10.1080/02726343.2021.1928375

[8] THARANI, D., BARIK, R. K., CHENG, Q. S., et al. Miniaturized SIW filter using D-shaped resonators with wide out-of-band rejection for 5G applications. *Journal of Electromagnetic Waves and Applications*, 2020, vol. 34, no. 18, p. 2397–2409. DOI: 10.1080/09205071.2020.1816219

[9] DONG, Y., YANG, T., ITOH, T. Substrate integrated waveguide loaded by complementary split-ring resonators and its applications to miniaturized waveguide filters. *IEEE Transactions on Microwave Theory and Techniques*, 2009, vol. 57, no. 9, p. 2211 to 2223. DOI: 10.1109/TMTT.2009.2027156

[10] CASSIVI, Y., PERREGRINI, L., ARCIONI, P., et al. Dispersion characteristics of substrate integrated rectangular waveguide. *IEEE Microwave Wireless Components Letters*, 2002, vol. 12, no. 9, p. 333–335. DOI: 10.1109/LMWC.2002.803188

[11] SANDHYA, R., ALI, U. H. H., CHENNIAPPAN, S. Compact dual mode X-band SIW bandpass filter with wide spurious suppression using split square ring slot resonator. *Circuit World*, 2020, vol. 48, no. 1, p. 1–13. DOI: 10.1108/CW-08-2019-0094

[12] DANAEIAN, M., GHAYOUMI-ZADEH, H. Miniaturized substrate integrated waveguide filter using fractal open complementary split-ring resonators. *International Journal of RF and Microwave Computer-aided Engineering*, 2018, vol. 28, no. 5, p. 1–10. DOI: 10.1002/mmce.21249

[13] LIU, Z., XIAO, G., ZHU, L. Triple-mode bandpass filters on CSRR-loaded substrate integrated waveguide cavities. *IEEE Transactions on Components, Packaging and Manufacturing Technology*, 2016, vol. 6, no. 7, p. 1099–1105. DOI: 10.1109/TCPMT.2016.2574562

[14] CHANG, K., KWAK, S. I., YOON, Y. J. Equivalent circuit modeling of active frequency selective surfaces. In *Proceedings of the IEEE Radio and Wireless Symposium (RWS)*. Orlando (USA), 2008, p. 663–666. DOI: 10.1109/RWS.2008.4463579

[15] SÁNCHEZ-SORIANO, M. Á., SIRCI, S., MARTÍNEZ, J. D., et al. Compact dual-mode substrate integrated waveguide coaxial cavity for bandpass filter design. *IEEE Microwave and Wireless Components Letters*, 2016, vol. 26, no. 6, p. 386–388. DOI: 10.1109/LMWC.2016.2558651

[16] CHENG, F., LIN, X. Q., LANCASTER, M. J., et al. A dual-mode substrate integrated waveguide filter with controllable transmission zeros. *IEEE Microwave and Wireless Components Letters*, 2015, vol. 25, no. 9, p. 576–578. DOI: 10.1109/LMWC.2015.2451362

[17] GU, L., DONG, Y. A compact, hybrid SIW filter with controllable transmission zeros and high selectivity. *IEEE Transactions on Circuits and Systems II-Express Briefs*, 2022, vol. 69, no. 4, p. 2051–2055. DOI: 10.1109/TCSII.2022.3144268

[18] SHEN, W., ZHU, H. Vertically stacked trisection SIW filter with controllable transmission zeros. *IEEE Microwave and Wireless Components Letters*, 2020, vol. 30, no. 3, p. 237–240. DOI: 10.1109/LMWC.2020.2969560

[19] LIU, Q., QIAN, H., ZHANG, D. F., et al. Compact highly-selective bandpass filter based on triple-mode ridge substrate integrated waveguide cavity. *IEEE Microwave and Wireless Technology Letters*, 2023, vol. 33, no. 9, p. 1274–1277. DOI: 10.1109/LMWT.2023.3276794

[20] ZHENG, Y., DONG, Y. Miniaturized hybrid filter using stripline and LC-loaded SIW resonators. *IEEE Transactions on Circuits and Systems II-Express Briefs*, 2022, vol. 69, no. 9, p. 3719–3723. DOI: 10.1109/TCSII.2022.3179393

About the Authors ...

Fatma Zohra HAMRIOUI (corresponding author) received her Master's degree in Telecommunications from the Institute of Electrical and Electronic Engineering (IGEE – formerly INELEC), M'hamed Bougara University of Boumerdès (UMBB), in 2020. She is currently a PhD student in Electronic Telecommunication Systems at the National Polytechnic School of Algiers (ENP), where she is affiliated with the LDCCP Laboratory. Her research interests lie in microwave circuits, specifically filters and antennas.

Rachida TOUHAMI obtained the diploma of engineer in Electronics and then the master's in Microelectronics, respectively, in 1985 and 1989 from the National Polytechnic School (ENP). After years of research devoted to the modeling of submicron structures MOS, she obtained the PhD degree in Microelectronics from the same school (ENP). She was promoted to the rank of professor at the Faculty of Electronics and Computer Science in 2006. Touhami is the author and co-author of several scientific publications in her field and currently she is interested in component-related instrumentation applications, working in microwave bands.

Mohamad AL SABBAGH received his B.S. degree in Electrical and Electronic Engineering from the University of Sharjah, UAE, in 2017. He then earned his M.S. degree in Electrical and Computer Engineering from the University of Ottawa, Canada, where he is currently pursuing a Ph.D. in the same field. He worked as a teaching assistant at the University of Sharjah from 2017 to 2018 and has been a teaching assistant at the University of Ottawa since 2018. His research focuses on mixed analog/digital IC design for wireless power transfer and energy harvesters in beamforming applications. Additionally, he investigates charge trapping and self-heating effects in GaN HEMT devices fabricated on various substrates and their impact on current dispersion. He is also developing novel extraction techniques for small-signal modeling of active devices. His research interests include microwave, RF, and mixed-signal IC design, wireless power transfer, energy harvesting, and transistor modeling.

Mustapha C. E. YAGOUB received the Dipl.-Ing. degree in Electronics and the Magister degree in Telecommunications, both from the École Nationale Polytechnique, Algiers, Algeria, in 1979 and 1987, respectively, the Ph.D. degree from the Institut Polytechnique de Toulouse - École Nationale Supérieure d'Electronique, d'Electrotechnique, d'Informatique et d'Hydraulique de Toulouse (INP-ENSEEIHT), Toulouse, France, in 1994, and the Doctorat d'état from the Université des Sciences et de la Technologie Houari Boumédiene (USTHB), Algiers, Algeria, in 1996. After few years working in industry as a design engineer, he joined the Institute of Electronics, USTHB, Algiers, Algeria, first as Lecturer during 1983–1991 and then as Assistant Professor during 1994–1999, holding the position of Head of the Communication Department from 1996 to 1999. From 1991 to 1994, he was seconded to INP-ENSEEIHT, working toward his Ph.D. From 1999 to 2001, he was a visiting scholar with the Department of Electronics, Carleton University, Ottawa, ON, Canada, working on neural networks applications in microwave areas. In 2001, he joined the School of Electrical Engineering and Computer Science, University of Ottawa, Ottawa, ON, Canada, where he is currently a Professor Emeritus. His research interests include wireless communication system design, RF/microwave CAD, RFID design, robotics, antenna design, active/passive device modeling and characterization, neural networks for high frequency applications, and applied electromagnetics. He has authored or coauthored over 600 publications in these topics in international journals and referred conferences. He also authored "Conception de circuits linéaires et non linéaires micro-ondes" (Cépadues, Toulouse, France, 2000). Dr. Yagoub is a senior member of the IEEE Microwave Theory and Techniques Society and a member of the Professional Engineers of Ontario, Canada.